Laser and Particle Beams (2003), *21*, 97–101. Printed in the USA.

DOI: 10.1017/S0263034603211186

Plasma properties of a laser-ablated aluminum target in air

MINJU YING,[1] YUEYUAN XIA,[2] YUMING SUN,[1] MINGWEN ZHAO,[2] YUCHEN MA,[1] XIANGDONG LIU,[2] YUFEI LI,[1] AND XUEYUAN HOU[1]

[1]Department of Optoelectronics, Shandong University, Jinan, Shandong, P.R.China
[2]Department of Physics, Shandong University, Jinan, Shandong, P.R.China

(RECEIVED 26 March 2002; ACCEPTED 11 November 2002)

Abstract

The optical emission spectra of the plasma generated by a 1.06-μm Nd:YAG laser irradiation of Al target in air was recorded and analyzed in a spatially resolved manner. Electron temperatures and densities in the plasma were obtained using the relative emission intensities and the Stark-broadened linewidths of Al(I) emission lines, respectively. The dependence of the electron density and temperature on the distance from the target surface and on the laser irradiance were manifested. We also discussed how the air takes part in the plasma evolution process and confirmed that the ignition of the air plasma was by the collisions between the energetic electrons and the nitrogen atoms through a cascade avalanche process.

Keywords: Laser-ablated aluminum; Optical emission; Electron density

1. INTRODUCTION

Plasmas produced by focusing laser beams onto solid targets have been the objects of intensive theoretical and experimental studies ever since high-power lasers became available (Radziemski & Cremers, 1989; Russo, 1995). The nature of the laser-induced plasma is itself an interesting field of study since it is rather difficult to model these events, especially when laser ablation is performed in the air, where a laser-supported detonation (LSD) wave is initiated either by the breakdown of the vaporized material or by the actual breakdown of the air above the surface. The study of laser-produced plasma also has important practical applications. The ablated material ejected from a target exposed to a high-power laser carries both mass and energy that can be used to form thin films. In fact, pulsed laser deposition (PLD) has been one of the most popular methods employed to fabricate thin films (Agostinelli *et al.*, 1993; Liu *et al.*, 1994). As the physical characteristics of the plasma play a crucial role in the microscopic mechanism of film growth, it is of great importance to get some quantitative information on the fundamental plasma parameters, such as electron temperature, electron density, and their spatial distribution, changing with the laser power density. Although various works have concentrated on this topic (Griem, 1964; Hughes, 1975; Bekfi, 1976; Harilal *et al.*, 1997; Gordillo-Vazquez *et al.*, 2001), the characterization of plasma is still a demanding field. In this article, we report the studies on plasma parameters of aluminum, such as the electron density and the electron temperature and their dependence on the incident laser irradiance and the spatial separation from the target surface. The ignition mechanism of the air plasma is also discussed.

Address correspondence and reprint requests to: Minju Ying, Department of Optoelectronics, Shandong University, Jinan, Shandong 250100 P.R. China.

2. EXPERIMENTAL SETUP

The experimental arrangement is shown in Figure 1.

The plasma was generated by ablating of a high-purity polycrystalline aluminum with 1.06-μm laser pulses from a Q-switched Nd:YAG laser (10 ns duration, YG-580, Quantel). A quartz lens (L_1) with a 10-cm focal length was used to focus the laser on the target. The spot size of the laser on the target is about 1 mm. The laser energy was monitored with a Joulemeter (Molectron, EPM1000). The sample and the focus lens were mounted on a three-dimensional movable plate. A cylindrical lens ($f = 4.8$ cm) was used to image the laser-induced plasma 1:1 onto the entrance slit of a spectrometer (spectrapro300i, Actron Research) with the slit width set to 10 μm. The spectra were recorded with a CCD

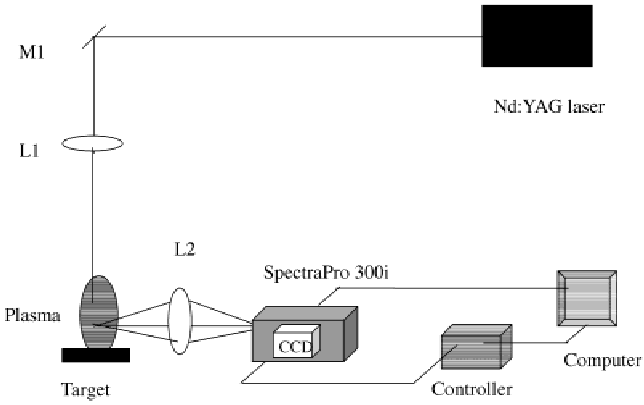

Fig. 1. Experimental setup for laser-induced plasma spectroscopy.

detector (100 × 1340 pixels, Princtron Instrument Inc.). By moving the plate with the target along the laser beam axis, the emission spectra from the plasma were recorded as a function of the distance from the target surface. The output was processed and stored via GPIB interface to a personal computer.

3. RESULTS AND DISCUSSION

One of the most powerful spectroscopic techniques to determine the electron density with reasonable accuracy is by the measurement of the Stark-broadened line profile of an isolated atom or singly charged ions. For non-hydrogen neutral atoms and singly ionized ions, the full-half widths $\Delta\lambda_{1/2}$ are related to the electron density by the expression (Bekfi, 1976)

$$\Delta\lambda_{1/2} = 2W\left(\frac{N_e}{10^{16}}\right) + 3.5A\left(\frac{N_e}{10^{16}}\right)^{1/4}[1 - 0.75N_D^{-1/3}]W\left(\frac{N_e}{10^{16}}\right)\text{ Å}, \quad (1)$$

for lines of neutral atoms,

$$\Delta\lambda_{1/2} = 2W\left(\frac{N_e}{10^{16}}\right) + 3.5A\left(\frac{N_e}{10^{16}}\right)^{1/4}[1 - 1.2N_D^{-1/3}]W\left(\frac{N_e}{10^{16}}\right)\text{ Å}, \quad (2)$$

for lines of singly ionized ions, where W and A are width parameters which can be found from Griem (1964), N_e is electron density in cm^{-3} and N_D is the number of particles in the Debye sphere defined as

$$N_D = \frac{4}{3}\pi N L_D^3 = 1.72 \times 10^9 \frac{[T(\text{eV})]^{3/2}}{[N(\text{cm})^{-3}]^{1/2}}.$$

Plasma density determinations through use of the Stark broadening of spectral lines is a well established and reliable technique in the range $10^{14} \leq N_e \leq 10^{18}$ cm^{-3}. For singly ionized helium lines, the electron density N_e can be determined to better than approximately 15% (Bekfi, 1976). However, for determining T_e accurately, spectroscopy has considerably less to offer compared to its potential as a probe of N_e, because the theories required in the interpretation of the measured quantities are fairly model dependent and sensitive to prevailing equilibrium conditions (e.g. local thermodynamic equilibrium vs. corona equilibrium; Bekfi, 1976). Under the assumption of local thermodynamic equilibrium (LTE), the electron temperature in the plasma can be determined by relative line intensity measurements. If one observes two isolated lines emanating from the same atomic or ionic species, say 1 and 2 with central wavelength $\lambda_0(1)$ and $\lambda_0(2)$, respectively, and if the level population are distributed according to the Boltzmann law, the relative intensity of these two lines can be written as (Bekfi, 1976)

$$\frac{\varepsilon_1}{\varepsilon_2} = \frac{f_{mn}(1)g_n(1)}{f_{mn}(2)g_n(2)}\left(\frac{\lambda_0(2)}{\lambda_0(1)}\right)^3 \exp^{-[(E_m(1)-E_m(2))/kT_e]}, \quad (3)$$

where $f_{mn}(i)$ $(i = 1,2)$ is the absorption oscillator strength for the transition m, n, $g_n(i)$ is the statistical weight of the lower level, $E_m(i)$ is the energy of the upper energy state m, k is the Boltzmann constant, and T_e is the electron temperature. From Eq. (3), the electron temperature T_e can be determined, provided f_{mn}, g_n, and E_m are known. The atomic spectra data needed in Eq. (3) can be found in Wiese *et al.* (1969).

In the present work, we used the Stark-broadened full width half maximum (FWHM) of Al(I) 396.15 nm to determine the electron density, and the relative line intensity of Al(I) 394.40 nm and 308.21 nm to evaluate the electron temperature. Figure 2a shows the spatial evolution of the Al(I) 394.40 nm and 396.15 nm resonant lines emitted from the plasma produced by a single laser pulse with power density of 3.8 GW/cm^2. From this figure, the Al(I) signals first increase and then decrease steadily after reaching a maximum around distance $d \sim 1$ mm. Also, it is clear that strong continuum emission is manifested. As the continuum is related to the strong collisions between the free electrons and the excited atoms and ions, known as bremsstrahlung, and the recombinations of electrons with ions, thus it can be concluded that there must be many electrons, excited atoms, and ions in the ejecting vapor. Figure 2a also shows clearly that the resonant spectral lines are substantially broadened. It is mainly due to Stark broadening caused by electron impacting (Bekfi, 1976). A typical Stark broadened line profile is approximately Lorentzian, and as an example, the experimentally measured Al(I) lines at 308.21 nm and 309.27 nm and their Lorentzian fits are shown in Figure 2b. It is evident that the experimentally measured lines can be fitted very well with two Lorentzian-shaped lines. From those lines the FWHM of the peaks, the integral intensities, the center wavelengths, and the continuum emission can be

https://doi.org/10.1017/S0263034603211186 Published online by Cambridge University Press

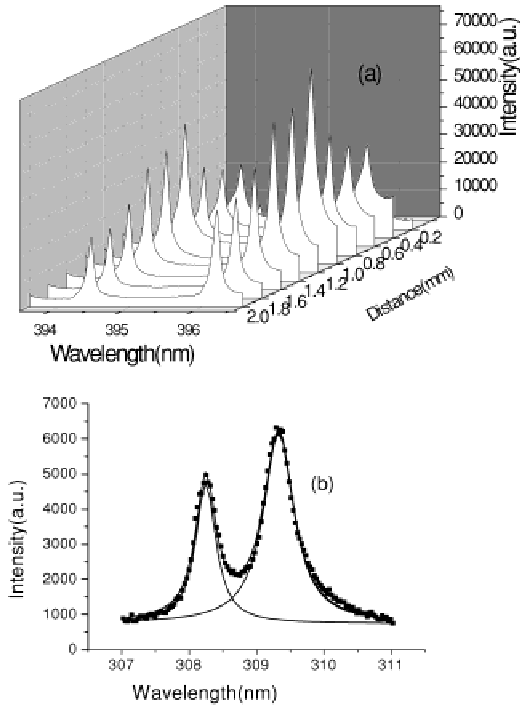

Fig. 2. Typical plasma spectra induced by a single pulse from a Nd:YAG laser irradiating an Al target. (a) The spatial evolution of Al(I) 399.40 nm and 396.15 nm resonant lines. Laser irradiance used is 3.8 GW/cm^2. (b) Typical Strark-broadened profiles of Al(I) 308.21 nm and 309.27 nm spectral lines. The solid line is a two-peak Lorentzian fit.

obtained. The electron density and the electron temperature of the plasma can be deduced using these parameters.

Figure 3 shows the spatial distribution of the integral intensities of the Al(I) 394.40 and Al(I) 396.15 nm resonant double lines, the N(II) 399.50 nm line, and the continuum spectrum integrated from 410.00 nm to 411.02 nm. As the spectral intensity of a specific atom or ion is proportional to the number density of the atom or ion in the upper excited state, the above integral intensity distributions reflect the spatial evolutions of the excited Al(I) atoms and N(II) ions. It also shows clearly that all the signals increase rapidly near the target surface, reach the maximum at a distance about 1 mm from the target surface, then decrease steadily with the increasing of the distance. The N(II) signal and the continuum emission have very similar spatial distributions and mainly exist in a range from 0 to 3 mm near the target surface.

Electron temperature and electron density of the laser-induced Al plasma as functions of distance from the target surface are shown in Figure 4a,b, respectively. The power density of the laser used is 3.8 GW/cm^2. As can be seen from the figure, the electron temperature and density decrease rapidly within a short distance from the target surface while at a longer distance they exhibit relatively little variation. With the increase in the distance from the target surface, the electron density falls from 1.12×10^{17} cm^{-3} at 0.4 mm to 0.68×10^{17} cm^{-3} at 2 mm while the electron temperature falls from 0.54 eV at 0.8 mm from the target to 0.40 eV at 2 mm. The variation of electron temperature with distance is slower than that of electron density. This is consistent with

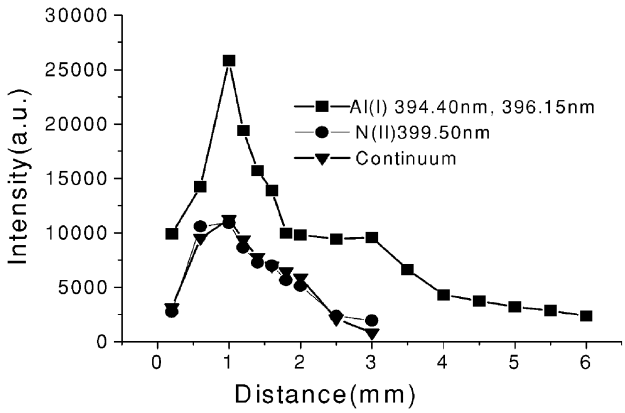

Fig. 3. The integral intensities of Al(I) 394.40 nm and 396.15 nm (■), N(II) 399.50 nm (●), and the continuum intensity integrated from 410.00 nm to 411.02 nm (▼), as a function of the distance from the target surface.

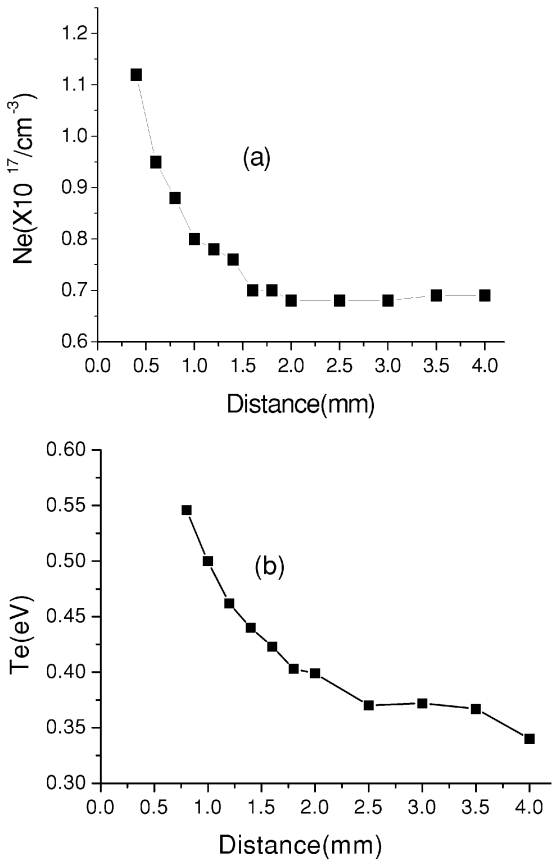

Fig. 4. (a) The electron density as a function of distance from the target surface. (b) The electron temperature as a function of distance from the target surface. Laser irradiance used is 3.8 GW /cm^2.

https://doi.org/10.1017/S0263034603211186 Published online by Cambridge University Press

the conclusions of Harilal *et al.* (1997) and Gordillo-Vazquez *et al.* (2001).

The calculation of electron temperature was carried out under the assumption that the plasma is in local thermodynamic equilibrium (LTE). In a transient system, such as the plasma formed by a pulsed laser beam, LTE is said to exist if the time between collisions of the particles in the plasma is small compared with the duration over which the plasma undergoes any significant change. When electron collisions are the major processes of de-excitation, the system is said to be at LTE (Harilal *et al.*, 1997). A necessary condition for LTE to be satisfied is (Bekfi, 1976)

$$N_e \geq 1.4 \times 10^{14} T_e^{1/2} (\Delta E_{mn})^3 \text{ cm}^{-3},$$

where T_e is the temperature in electron volts and ΔE_{mn} is the energy difference between the upper and the lower energy level in electron volts. For the transition of Al(I) 308.21 nm, $\Delta E_{mn} = 4.02$ eV, according to the temperature given above, the lowest limit for N_e is 6.46×10^{15} cm^{-3}. Our calculated results of N_e are much higher than this value. This means that the LTE assumption seems valid.

The two dominant mechanisms responsible for plasma absorption at the laser irradiance used in the present work are inverse bremsstrahlung absorption and photoionization. As the photoionizaton process is dominant only in the visible and the ultraviolent laser light case, inverse bremsstrahlung absorption may be the prevailing plasma absorption mechanism in the present experiment. The inverse bremsstrahlung absorption coefficient α via free electrons is approximated by (Bekfi, 1976)

$$\alpha(m^{-1}) = 7.01 \times 10^{-11} \frac{N^2 Z}{T^{3/2} \omega^2} \left[\frac{1 - e^{-\hbar\omega/kT}}{\hbar\omega/kT} \right] G_{ff}, \qquad (4)$$

where G_{ff} is the gaunt factor, which is assumed to be unity by Kramer's rule (Spitzer, 1962). Take N_e as 1.0×10^{17} cm^{-3}, T_e as 0.50 eV, from the above equation, $\alpha \approx 0.19$ m^{-1}. As in our experiment, the transversal expansion of the plasma l is about 2 mm, so $\alpha l = 3.88 \times 10^{-4}$. This confirms that the absorption is negligible and the plasma can be regarded as optically thin.

The nature and characteristics of a laser-induced plasma strongly depend on the laser irradiance condition. Figure 5a,b shows the variations of the electron temperature and the electron density, respectively, for the laser-induced Al plasma with respect to laser power density at a fixed distance of 0.5 mm from the target surface. As the laser irradiance increases from 1.39 GW/cm^2 to 3.82 GW/cm^2, the electron temperature increases from 0.24 eV to 0.41 eV, and then only increases very slowly. In the same irradiance range, the electron density varies from 1.03×10^{17} cm^{-3} to 1.12×10^{17} cm^{-3}, and then remains almost constant. This may be due to the plasma shielding effect, that is, absorption and/or reflection of the laser photons by the plasma. As the ablation was performed in air, the air plasma may absorb

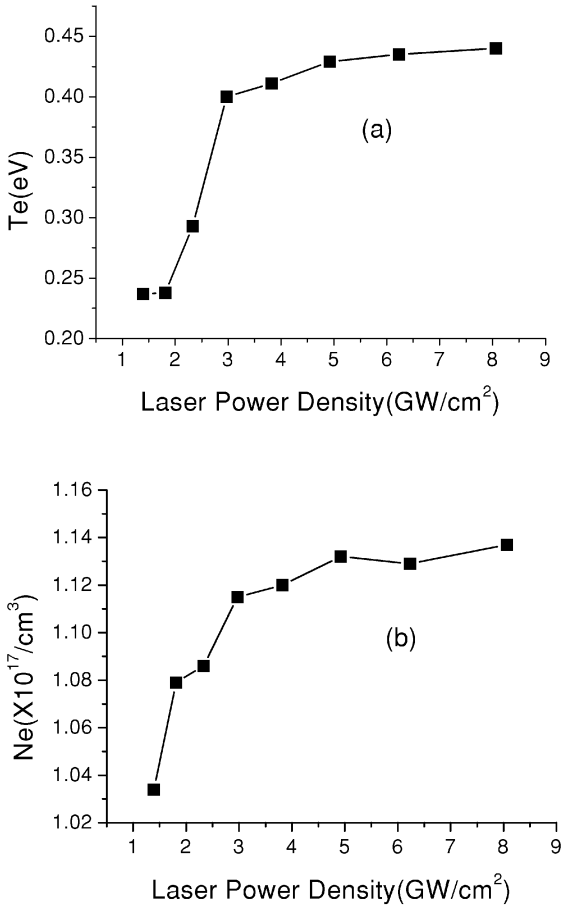

Fig. 5. (a) The variation of electron temperature with laser irradiance. (b) The variation of electron density with laser irradiance. The distance is fixed at 0.5 mm from the target surface.

part of the laser energy and decrease the efficiency of the laser available for ablation of the target material. To better understand the effect of the air plasma, we give the intensities of the spectral lines emitted from Al(I) 394.40 nm, N(II) 399.50 nm, and the continuum, respectively, as functions of laser irradiance, in Figure 6. The continuum was obtained by two-peak Lorentzian fit of Al(I) 399.40 and Al(I) 396.15 nm resonant lines. From the figure, it is obvious that at a high irradiance level, the Al signal does not increase very much with the increase of laser power density, while the continuum signal and the N(II) signal increase remarkably with the laser power density. When the laser power is low (less than 3 GWcm^{-2}), the Al signal increases quickly. As the laser power density is greater than 3 GW/cm^2, the Al signal increases only quite slowly. The N(II) signal increases exponentially ($\alpha \exp(0.33\phi)$. This means that the number density of excited Al atoms increases slowly because of the plasma absorption and shielding effect at high power density.

As we have observed that the N(II) signal is much stronger than the O(II) signal, Smith *et al.* (1972) also pointed out that the nitrogen atom and molecular were more impor-

https://doi.org/10.1017/S0263034603211186 Published online by Cambridge University Press

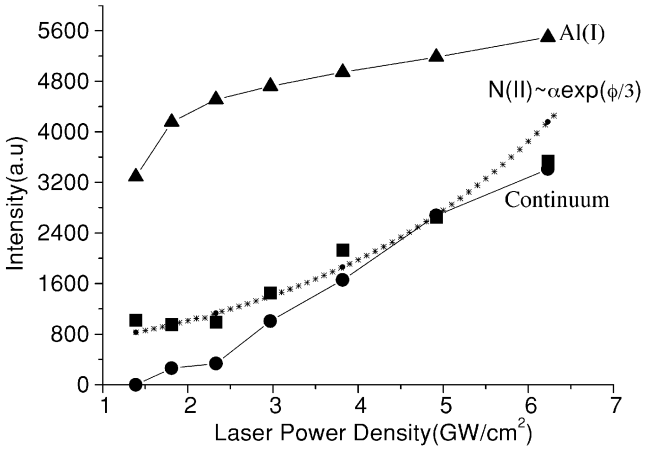

Fig. 6. Intensity variations of Al(I) 394.40 nm, N(II) 399.50 nm, and continuum emission with laser power density. The stars (*) are the exponential fit to the intensity of N(II).

tant than the oxygen atom and molecular. Thus the study of the mechanism for N(II) formed in the plasma is essential for understanding the air breakdown induced by the high-power laser in air background. As the laser we used here is 1.06 μm, avalanche cascade ionization may be preferred over the photoionization process for causing the air breakdown because the latter is dominant only in the visible and ultraviolet laser light case. In the intense laser light field, a free electron can gain sufficient energy through inverse bremsstrahlung absorption, and the energetic electrons will ionize the atoms by collisions between the electrons and atoms. Thus the number of electrons doubles in a certain characteristic time and a cascade process develops, causing an exponential growth of ionization. According to Haughes's (1975) simple model describing the cascade process, the final electron density $N_e \propto \exp(t_p I/A)$; here t_p is the effective laser pulse duration, and A is a parameter related to the laser angular frequency and the collision frequency between electrons and atoms. This equation predicts an exponential dependence of N_e on I.

If the cascade process is dominant as suggested above, the final number density of N(II) in the plasma should be approximately proportional to the electron density N_e, which has a exponential dependence on I, since the density of N(II) in the air plasma is much higher than the components of O(II) and other ion species, which may stem from the components of air background. Therefore the intensity of N(II) line proportional to the density of N(II) should increase exponentially with the laser intensity I, which is consistent with the experimental result shown in Figure 6.

This result and the result shown in Figure 3 confirm that the ignition of the air plasma is mainly due to the collisions between the electrons and the nitrogen atoms via a cascade avalanche process. Many facts support this conclusion. First, the emission intensity from N(II) line increases exponentially with laser intensity. This coincides with the cascade theory (Haughes, 1975). Second, the N(II) signal co-exits spatially together with the continuum spectrum, which stems from the bremsstrahlung process, as shown in Figure 3. Third, many authors (Man *et al.*, 1997) have proved that the nitrogen ions in the plasma do not have a traveling velocity toward the laser source, which means that the ionization process of nitrogen atoms does not involve large momentum exchange, that is to say, the ionization process must take place between electrons and much heavier nitrogen atoms.

4. CONCLUSIONS

We performed laser ablation of an Al target under air atmosphere using a 1.06-μm Nd:YAG laser. The spectra were recorded and analyzed in a spatially resolved manner. The dependence of the electron density and temperature on distance from the target surface and on laser irradiance were manifested. Also we have discussed how the air takes part in the plasma evolution process and confirmed that the ignition of the air plasma is by collisions between the emitted electrons and nitrogen atoms through a cascade avalanche process.

REFERENCES

Agostinelli, J.A., Braunstein, G.H. & Blanton, T.N. (1993). *Appl. Phys. Lett.* **63**, 123.
Bekfi, G. (1976). *Principles of Laser Plasma*. New York: Wiley.
Gordillo-Vazquez, F.J. *et al.* (2001). *Appl. Phys. Lett.* **78**, 7.
Griem, H.R. (1964). *Plasma Spectroscopy*. New York: McGraw-Hill.
Harilal, S.S. *et al.* (1997). *J. Appl. Phys.* **82**, 2140.
Haught, A.F. & Polk, D.H. (1966). *Phys. Fluids* **9**, 2047.
Hughes, T.P. (1975). *Plasma and Laser Light*. Adam Hilger Ltd.
Liu, J.M. *et al.* (1994). *Appl. Phys. Lett.* **65**, 1995.
Man, B.Y. *et al.* (1997). *Chinese Science Bulletin* **42**, 997.
Mcwhirter, R.W. (1976). In *Plasma Diagnostic Techniques* (Huddlestone, R.H. & Leonard, S.L., Eds.). New York: Academic.
Radziemski, L.J. & Cremers, D.A., Eds. (1989). *Laser-induced Plasmas and Applications*. New York: Marcel Dekker.
Russo, R.E. (1995). *Appl. Spectrosc. A* **14**, 49.
Smith, D.C. *et al.* (1972). *Investigations of Gas Breakdown With 10.6 Micro Wavelength Radiation*. Technical Report AFWL-TR-72-182, United Technologies Research Center.
Spitzer, L. (1962). *Physics of Fully Ionized Gases*, 2nd Ed. New York: John Wiley & Sons.
Wiese, R.W. et al. (1969). *Atomic Transition Probabilities*. Washington, DC: National Standard Data Series.

https://doi.org/10.1017/S0263034603211186 Published online by Cambridge University Press